On a Conservative Solution to Checkerboarding: Examining the Causes of Non-Physical Pressure Modes

J.A. Hopman[*,1], **À. Alsalti-Baldellou**[1,2], **F.X. Trias**[1] **and J. Rigola**[1]

[1]Heat and Mass Transfer Technological Center, Technical University of Catalonia, ESEIAAT, c/Colom 11, 08222 Terrassa, Spain, jannes.hopman@upc.edu
[2]Termo Fluids SL, Sabadell (Barcelona), Spain; www.termofluids.com

1 Introduction

CFD codes used for industrial applications often apply a collocated grid arrangement. Consistently applying the central differencing scheme to discretise the Navier-Stokes equations in this arrangement leads to a wide-stencil Laplacian, in which odd and even cells are decoupled. This decoupling can result in high frequency, non-physical pressure modes, that lie on the kernel of the discrete Laplacian operator, commonly known as the checkerboard problem [Ferziger et al., 2002].

To avoid this problem and to decrease computational cost, a compact-stencil Laplacian is often applied for industrial purposes. This couples neighbouring cells and eliminates the checkerboard problem, at the cost of introducing numerical dissipation of kinetic energy [Rhie and Chow, 1983, Felten and Lund, 2006]. This dissipation disrupts the accurate capturing of the motion of fluids, especially at the smallest scales of turbulence [Verstappen and Veldman, 2003], and has been shown to be of a similar order of magnitude as applied LES models, decreasing their effectiveness [Komen et al., 2021].

Another possibility to eliminate the checkerboard problem is to filter the pressure solution from the pressure modes that lie on the kernel of the Laplacian operator [Larsson and Iaccarino, 2010]. After examining the existence and form of this kernel with respect to the mesh and discretisation method [Hopman et al., 2022], a logical follow-up question arose: *Does the existence of a non-trivial Laplacian kernel always lead to checkerboarding or are there additional requirements?*

To address this question, a close examination of the involved computational steps was made and three possible mechanisms were identified. These mechanisms were analysed using simple numerical tests.

Algorithm 1: Fractional step method (wide & compact stencil)

1. Predictor velocity:
$$\mathbf{u}_c^p = \mathbf{u}_c^n - \Delta t \Omega^{-1} \left(C\left(\mathbf{u}_s^n\right) + D \right) \mathbf{u}_c^n \tag{A 1.1}$$
2. Poisson equation:
   - **if** wide stencil **then**:
$$L_c \tilde{\mathbf{p}}_c^{n+1} = M_c \mathbf{u}_c^p \tag{A 1.2}$$
   - **else if** compact stencil **then**:
$$L \tilde{\mathbf{p}}_c^{n+1} = M_c \mathbf{u}_c^p \tag{A 1.3}$$
3. Update cell-centered velocities
$$\mathbf{u}_c^{n+1} = \mathbf{u}_c^p - G_c \tilde{\mathbf{p}}_c^{n+1} \tag{A 1.4}$$
4. Update face-centered velocities:
   - **if** wide stencil **then**:
$$\mathbf{u}_s^{n+1} = \Gamma_{cs} \mathbf{u}_c^{n+1} \tag{A 1.5}$$
   - **else if** compact stencil **then**:
$$\mathbf{u}_s^{n+1} = \Gamma_{cs} \mathbf{u}_c^p - G \tilde{\mathbf{p}}_c^{n+1} \tag{A 1.6}$$

2 Possible causes of checkerboarding

Following the notation of [Trias et al., 2014]. The discrete Navier-Stokes equations were solved using the fractional step method. Algorithm 1 illustrates this method using Forward Euler time-integration, as an example. In this method $L_c = M_c G_c = M\Gamma_{cs}\Gamma_{sc}G$ is the so-called wide-stencil Laplacian operator and, if chosen consistently, the interpolators are related by:

$$\Gamma_{sc} = \Omega^{-1}\Gamma_{cs}^{T}\Omega_s. \tag{1}$$

This only leaves one degree of freedom, the choice of collocated-to-staggered interpolator, Γ_{cs}. Conversely, equation (A 1.3) uses a compact-stencil Laplacian, $L = MG$. This eliminates the checkerboard problem at the cost of numerical dissipation related to non-zero divergence of the collocated velocities. Using this method, three different possible origins for the checkerboard problem were identified.

Mechanism 1. When using the compact-stencil method and letting $\Delta t \to 0^+$, the effect of the second term on the RHS of step (A 1.1) diminishes until $\mathbf{u}_c^p = \mathbf{u}_c^n$. This situation leads to:

$$\mathbf{u}_c^n = \mathbf{u}_c^{n-1} - G_c\tilde{\mathbf{p}}_c^n = \mathbf{u}_c^0 - G_c\sum_i^n \tilde{\mathbf{p}}_c^i \tag{2}$$

$$L\tilde{\mathbf{p}}_c^{n+1} = M_c\mathbf{u}_c^0 - L_c\sum_i^n \tilde{\mathbf{p}}_c^i \tag{3}$$

$$L\check{\mathbf{p}}_c^{n+1} = M_c\mathbf{u}_c^0 + (L - L_c)\,\check{\mathbf{p}}_c^n \tag{4}$$

in which $\check{\mathbf{p}}_c^n = \sum_i^n \tilde{\mathbf{p}}_c^i$. This gives a solution to equation (A 1.3) which can contain checkerboard modes that lie on the kernel of L_c, even though a compact-stencil Laplacian is used.

Mechanism 2. The second method involves the choice in Poisson solver. For a stationary iterative method and the compact-stencil Laplacian, the Poisson equation is solved as:

$$\tilde{\mathbf{p}}_c^{n+1} = \sum_{i=0}^{k}\left(I - \bar{L}^{-1}L\right)^i \bar{L}^{-1}M_c\mathbf{u}_c^p + \left(I - \bar{L}^{-1}L\right)^{k+1}\tilde{\mathbf{p}}_c^n \tag{5}$$

where $\bar{L}$ is the invertible part of L, after splitting the matrix into an invertible and a non-invertible part as: $L = \bar{L} + \hat{L}$, e.g. $\bar{L} = diag(L)$ for the Jacobian method. The second term on the RHS of equation (5) accounts for the initial guess and is optional. If the image of $\bar{L}^{-1}$, $\mathrm{Im}\left(\bar{L}^{-1}\right)$, is non-orthogonal to the kernel of L_c, $\mathrm{Ker}\left(L_c\right)$, the solution can contain checkerboard modes. These modes can subsequently be preserved by the implementation of the initial guess. Similarly, if a preconditioner is used as:

$$Q_L^{-1}LQ_R^{-1}\tilde{\mathbf{q}}_c^{n+1} = Q_L^{-1}M_c\mathbf{u}_c^p \tag{6}$$

where $Q_R^{-1}\tilde{\mathbf{q}}_c^{n+1} = \tilde{\mathbf{p}}_c^{n+1}$, then $\mathrm{Im}\left(Q_R^{-1}\right)$ might not be orthogonal to $\mathrm{Ker}\left(L_c\right)$, possibly leading to checkerboarding.

Mechanism 3. The third method involves the wide-stencil Laplacian that is implicitly formed by the divergence and gradient, M_c and G_c, on the RHS of equations (A 1.2), (A 1.3) and (A 1.4). If both interpolations in these operators are consistent, e.g. both midpoint, we can show that this operation is symmetric:

$$M_cG_c = M\Gamma_{cs}\Gamma_{sc}G = M\Gamma_{sc}\Omega^{-1}\Gamma_{cs}^{T}\Omega_sG = -M\Gamma_{sc}\Omega^{-1}\Gamma_{cs}^{T}M^T \tag{7}$$

where we used $G = -\Omega_s^{-1} M^T$. For symmetric matrices the image and kernel are orthogonal, i.e. $L_c^T = L_c \rightarrow \mathrm{Im}(L_c) \perp \mathrm{Ker}(L_c)$, if not, the result of this operation can contain checkerboard modes. This implicit $M_c G_c$ occurs when rewriting RHS of equation (A 1.2) and (A 1.3) using equations (A 1.1) and (A 1.4):

$$M_c \mathbf{u}_c^p = M_c \mathbf{u}_c^{p-1} - M_c G_c \tilde{\mathbf{p}}_c^n - \Delta t M_c \Omega^{-1} \left(C\left(u_s^n\right) + D \right) \mathbf{u}_c^n. \tag{8}$$

Therefore, checkerboarding might arise if the interpolators in G_c and M_c are chosen to be inconsistent with respect to each other, i.e. not according to equation (1).

3 Numerical results

To test the different mechanisms, a two-dimensional Taylor-Green vortex was used. Different parameters were varied to examine their influence on checkerboarding, such as viscosity (ν), Laplacian discretisation, mesh stretching and Poisson solver. Only by using the mechanisms that were mentioned, was it possible to produce checkerboarding, see figure 1. By analysing a wide variety of cases, a deeper insight into the cause of checkerboarding will be provided.

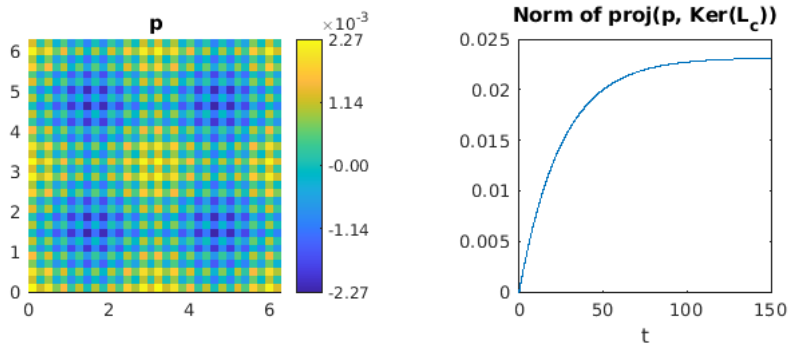

Figure 1: Taylor-Green vortex on a uniform grid, with $\nu = 0.01$ and using a pCG solver for Cholesky factorisation of the wide-stencil Laplacian. Pressure (left) and norm of checkerboard modes (right).

References

[Felten and Lund, 2006] Felten, F. N., & Lund, T. S. (2006). Kinetic energy conservation issues associated with the collocated mesh scheme for incompressible flow. Journal of Computational Physics, 215(2), 465-484.

[Ferziger et al., 2002] Ferziger, J. H., Perić, M., & Street, R. L. (2002). Computational methods for fluid dynamics (Vol. 3, pp. 196-200). Berlin: springer.

[Hopman et al., 2022] Hopman, J. A., Trias, F. X., Rigola, J. (2022). On a conservative solution to checkerboarding: Examining the discrete Laplacian kernel using mesh connectivity. Proceedings of the 13th International ERCOFTAC Workshop on Direct and Large-Eddy Simulation (DLES12), Held at the University of Udine, October 2022.

[Komen et al., 2021] Komen, E. M., Hopman, J. A., Frederix, E. M. A., Trias, F. X., & Verstappen, R. W. (2021). A symmetry-preserving second-order time-accurate PISO-based method. Computers & Fluids, 225, 104979.

[Larsson and Iaccarino, 2010] Larsson, J., & Iaccarino, G. (2010). A co-located incompressible Navier-Stokes solver with exact mass, momentum and kinetic energy conservation in the inviscid limit. Journal of Computational Physics, 229(12), 4425-4430.

[Rhie and Chow, 1983] Rhie, C. M., & Chow, W. L. (1983). Numerical study of the turbulent flow past an airfoil with trailing edge separation. AIAA journal, 21(11), 1525-1532.

[Trias et al., 2014] Trias, F. X., Lehmkuhl, O., Oliva, A., Pérez-Segarra, C. D., & Verstappen, R. W. C. P. (2014). Symmetry-preserving discretization of Navier–Stokes equations on collocated unstructured grids. Journal of Computational Physics, 258, 246-267.

[Verstappen and Veldman, 2003] Verstappen, R. W. C. P., & Veldman, A. E. P. (2003). Symmetry-preserving discretization of turbulent flow. Journal of Computational Physics, 187(1), 343-368.